P2.4 CERES PROTO-EDITION3 RADIATIVE TRANSFER: MODEL TESTS AND RADIATIVE CLOSURE OVER SURFACE VALADATION SITES

Fred Rose*, Thomas Charlock, Qiang Fu, Seiji Kato, David Rutan, and Zhonghai Jin

1. Introduction

The Langley Fu-Liou Proto-Edition 3 code is a two-stream or four-stream or gamma weighted two-stream shortwave and a 2/4 stream longwave using correlated-k's. The original Fu-Liou code contained only six (6) broad shortwave bands. Modifications have expanded this to eighteen (18). Earlier modifications (c1996) divided the 0.25–0.70μ band into ten (10) bands to improve treatment of rayleigh scattering, aerosols and ozone. The latest modifications are in the 0.69-1.9 micron near-ir region.

#	Wavelength (microns)	Gases	# k
1	0.175-0.224	O_3	1
2	0.224-0.243	O_3	1
3	0.243-0.285	O_3	1
4	0.285-0.298	O_3	1
5	0.298-0.322	O_3	1
6	0.322-0.357	O_3	1
7	0.357-0.437	O_3	1
8	0.437-0.497	O_3, H_2O	1
9	0.497-0.595	O_3, H_2O	1
10	0.595-0.689	O_2, O_3, H_2O	1
11	**0.690-0.794**	**H_2O, O_2, O_3**	**8**
12	**0.794-0.889**	**H_2O**	**6**
13	**0.889-1.042**	**H_2O**	**8**
14	**1.042-1.410**	**H_2O**	**7**
15	**1.410-1.905**	**H_2O, CO_2**	**8**
16	1.905-2.500	H_2O, CO_2, CH_4	7
17	2.500-3.509	H_2O, CO_2, O_3, CH_4	8
18	3.509-4.000	H_2O, CO_2, CH_4	7

Table 1. The Ed3 Fu-Liou code band boundaries, gases treated and number of correlated k's absorption coefficients used per band, recently added bands in bold type.

This code is the proto-type for the Clouds and Earth's Radiant Energy System (Wielicki 1996) Surface Atmosphere Radiation Budget (CERES SARB) Edition3 radiative transfer products. Edition 3 will be a general CERES reprocessing, and the SARB component will use as inputs GMAO Geos 4.0.3 temperature and humidity profiles, SMOBA ozone, MODIS (CERES) derived cloud and aerosol products and MATCH (Collins 2001) aerosol vertical profiles and constituents types tied to OPAC scattering properties. Untuned and tuned fluxes are offered; tuned inputs are adjusted to bring modeled fluxes in closer agreement to observed CERES shortwave and longwave TOA fluxes. As a test of the code we show comparisons of model calculations over a more than 5 year period (March 2000 to June 2005) for a subset of instantaneous CERES FOV data over select locations where surface flux measurements are available.

*Corresponding author address: Fred G. Rose, Analytical Services and Materials (AS&M) 300 Enterprise Pkwy, Hampton, Va. 23666; e-mail: f.g.rose@larc.nasa.gov

2. Radiative Transfer Code

In this modification of the Fu-Liou code we retain many aspects of the code used in the recent CERES SARB Edition 2 (Charlock et al, 2006, on the archived, ungridded CRS Edition 2, Rutan et al, 2006, on a spinoff, gridded surface albedo product based on CRS Edition 2, and a second Rose et al, 2006, about work in progress on the developing, gridded SYNI Edition 2; all in this volume). These include sources of optical properties for water clouds (Hu 1993), ice clouds (Fu 1996) and aerosols [OPAC (Hess 1999), Tegin & Lacis (1996) ,d'Almedia (1991)]. Rayleigh scattering coefficients are taken from those in Modtran (Shettle 1980). Gas absorption is based on HITRAN 2000 restructured into sets of correlated k coefficients dependent on gas mixing ratio, pressure and temperature according to the method described by Kato (1999). And as in Edition2, we employ a Gamma Weighted Two Stream Algorithm (GWTSA) solver for shortwave; this models horizontal inhomogeniety in the cloud optical depth domain as a gamma distribution, using inputs of a linear and a log averaged optical depth (Kato 2005).

The original 0.69-1.3 μm band was broad containing roughly 35% of toa insolation. Even though it had 8 "k" gas absorption coefficients, unresolved spectral variability in Rayleigh, cloud and surface optical properties limited mean accuracy to about 1%. Within this large band rayleigh optical depth decreases by about an order of magnitude. Water vapor absorption is highly variable with almost none near 0.7μm, where Rayleigh is still significant; conversely in the longer portion of the band near 1.3 μm Rayleigh becomes insignificant while water vapor absorbs strongly.

Water cloud optical properties have a modest change across the 0.7-1.3 μ and 1.3-1.9 μ bands. Extinction (β/IWC) increases a few percent over the interval [0.69 -1.3]. Co-albedo has a large relative percentage change but is insignificant in

absolute magnitude. Asymmetry parameter (g) varies across this range by about 1% relative.

Ice clouds begin to show some absorption near 1.4 um, especially for large crystals. In the original implementation (Fu 1996) band mean optical properties for 0.7-1.41 were applied to the 0.7-1.3 band, causing a minor overestimate of absorption. This has been cleared up in the process of increasing the spectral resolution.

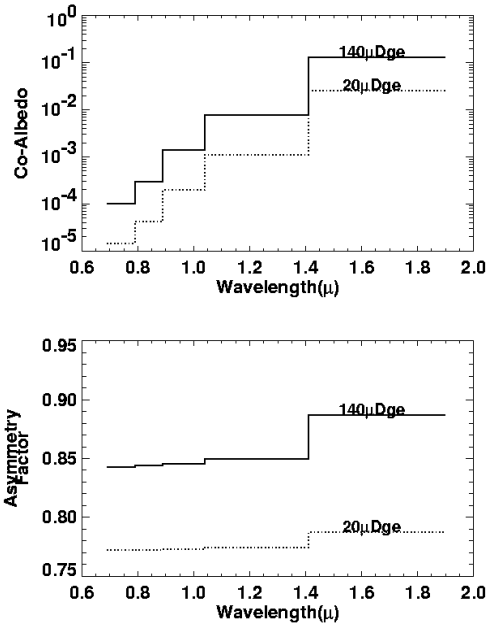

Fig 1. Plots of spectrally dependent Co-Albedo (1-ω), Asymmetry parameter (g) for new near-ir Fu-Liou bands for two particle sizes 20μ &140μ. Shows wavelength variability, some of which was not captured in earlier 0.7-1.3 & 1.3-1.9 micron bands.

Surface albedo for some surface types display very large spectral changes in the 0.69-1.90 micron range. The increased resolution helps model this radiative impact. For example a fresh snow surface has a large decrease in spectral albedo from 0.7 to 1.3μm

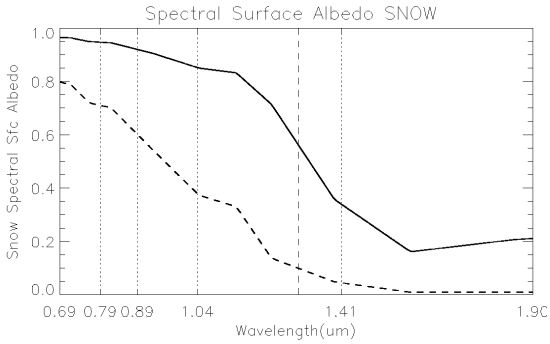

Fig 2. Example of spectral surface albedo of fresh snow (Solid) 50μ grain size and old snow (dashed) 2000μ grain size based on COART.

3. Model Tests

A suite of tests comparing this version of the Fu-Liou code against 1) An earlier version of the code 2) Coupled Ocean Atmosphere Radiative Transfer COART (Jin 1994) a high order discrete ordinate code were made for a range of solar zenith angles, cloud (phase, particle size, optical depth) and aerosol (type, optical depth) were made. Outputs examined were TOA reflected flux, surface downwelling flux and atmosphere absorbed flux.

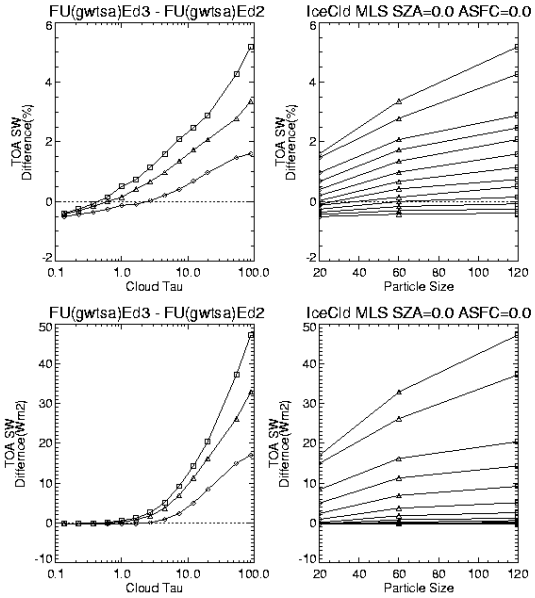

Fig 2. Comparison made between Fu-protoEd3 GWTSA and earlier version FuEd2 GWTSA showing TOA SW flux differences for ice clouds of various particle sizes (diameters of 20μm as diamonds, 60μm as triangles, and 120μm as squares) and optical depths for a solar zenith angle of 0 deg and a surface albedo of 0.

This new version of the code has significantly less ice cloud absorption for both large ice particles (Dge > 100) and large cloud optical depths ($\tau > 60$). Percent differences were greatest at small solar zenith angles, for which the TOA SW reflected increased by ~4%, SFC SW down increased by ~10%, and atmosphere absorbed decreased by ~10%. For liquid phase clouds, such changes were less than 2 % in all cases.

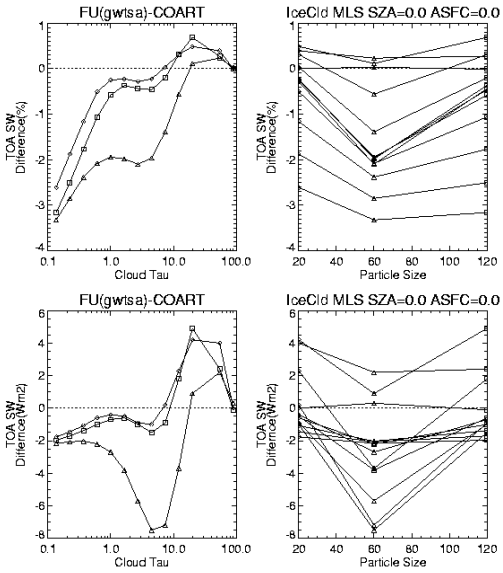

Fig 2. Example of model tests made between FuEd3 GWTSA code and COART showing TOA SW flux differences for ice clouds of various particle sizes and optical depths for a solar zenith angle of 0 deg and a surface albedo of 0.

4. Toa & Surface Validation

Data from 50 locations where surface flux measurements of broadband shortwave and longwave flux which also had CERES Terra instantaneous FOV observations of TOA fluxes, typically twice daily were used to validate model flux calculation. Model calculations used GEOS 4.0.3 assimilated temperature and humidity profiles, SMOBA ozone, CERES MODIS cloud property retrievals; MODIS based aerosol optical depths, MATCH aerosol constituents tied to OPAC optical properties. MATCH is also used for vertical aerosol profiles. Surface spectral emissivity and albedo *shape* are tied to IGBP type. Broadband surface albedo for clear sky cases is retrieved using CERES TOA shortwave and a model based atmospheric correction look-up-table. Cloud sky surface albedo is the monthly minimum clear sky value moved to the diffuse angle. Clear sky skin temperature is based on MODIS 11μ radiance; cloudy sky skin temperature is from GEOS.

It should be noted here CERES flux data is from Edition 2B CRS data that has ***not*** *been corrected for apparent SW UV darkening aka Rev1_correction (see Poster 3.12 Matthews)*

For the ARM SGP E13 site agreement, in the mean between model and observations, is good. SW TOA within 0.6 Wm^{-2}, however there is compensation of errors at low and high flux values. OLR bias is 2.4 Wm^{-2}, SFC SW DN 4.8 Wm^{-2} and SFC DLF showing the largest discrepancy at –6.0 Wm^{-2}. Downwelling longwave is highly sensitive to the lower atmosphere temperature and humidity as well as cloud base that is not sensed directly by the TOA based cloud property retrievals. The large RMS error of the instantaneous measurements shows some of the issues of instantaneous TOA flux accuracy, cloud property retrieval and scale mismatch of surface observations to FOV size.

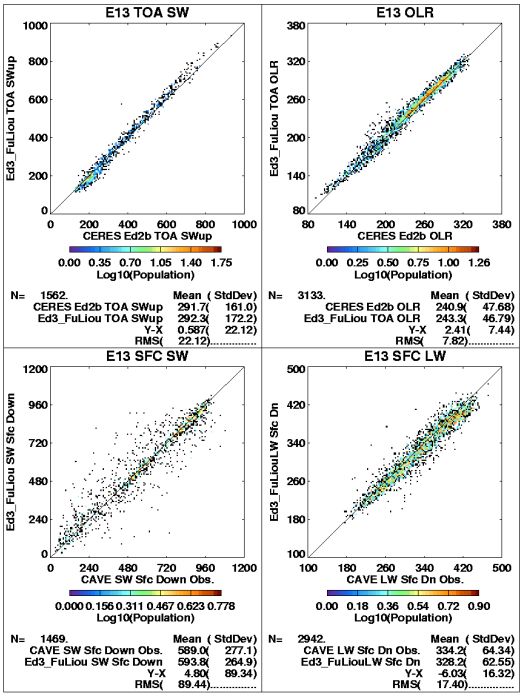

Fig 4. Scatterplots of proto-Ed3 Fu-Liou model Vs. Observations. Upper left) Shortwave Reflected TOA, upper right) outgoing Longwave TOA, lower left) Shortwave downwelling at SFC, lower right) Longwave downwelling at surface: over 5+ years of twice daily instantaneous at ARM SGP central facility. (Observations: FOV at TOA, 30min avg at sfc.)

While there is close agreement of these Edition3 computations at SGP, some of the other sites particularly coastal sites *see table 2* (BER, COV, TAT) show TOA SW biases where the 10' grid scale (~18km) cloudy sky broadband surface albedo used, was not representative of the closest FOV to each site. The biases of shortwave surface downwelling show large variability partly due to the scale mismatch of the surface measurement particularly during partly cloudy and cloudy sky conditions. The measurement scale of a TOA FOV is typically on order of 30+ km while the surface measurement scale is much smaller on order of 1km. Averaging of surface measurements to 30 minutes is done to compensate for some of the scale mismatch. Biases and standard deviations of Clear Sky are smaller.

An extensive set of validations including clear, cloudy sky with plots and tables for individual stations for Edition2 Ceres SARB CRS data can be found at the CAVE web site. Online Radiative transfer using the Langley Fu-Liou code and COART can also be found. ***http://snowdog.larc.nasa.gov/cave/***

Station	SWTOA (mean)	SWTOA (StdDev)	OLR (mean)	OLR (StdDev)	SWSfcDn (mean)	SWSfcDn (StdDev)	LWSfcDn (mean)	LWSfc Dn (StdDev)
Fort Peck, Mt FPK	5.2	19.5	1.4	6.7	11.8	87.9	-8.1	18.8
Penn State, Pa PSU	8.7	23.9	1.8	7.4	3.3	109.6	-2.6	16.7
Bondville, Il BON	2.4	28.6	1.5	7.3	6.2	84.3	-1.5	16.0
Table Mountain, Co TBL	0.2	24.3	-0.4	8.1	8.5	140.9	-17.5	17.0
Desert Rock, Nv DRA	3.9	15.7	-1.0	6.2	-1.5	79.2	-23.1	13.0
Goodwin Creek, Ms GWN	5.9	24.3	1.3	7.8	20.9	98.2	-4.2	13.7
Sioux Falls, Sd SXF	3.2	25.5	2.5	7.7	7.1	85.7	-2.4	18.7
ARM SGP E01	1.2	21.7	1.6	7.0	8.0	89.5	-3.8	16.4
ARM SGP E02	4.5	21.5	2.0	7.1	12.6	82.6	-5.4	17.6
ARM SGP E03	6.5	23.9	1.8	7.4	11.3	83.6	-8.7	15.5
ARM SGP E04	2.2	20.6	2.4	7.0	12.3	79.8	-3.8	15.6
ARM SGP E05	3.3	20.4	2.0	7.1	8.6	73.1	-6.5	15.4
ARM SGP E06	5.4	21.1	2.5	7.0	8.8	78.7	-0.7	15.6
ARM SGP E07	6.4	20.7	2.0	7.3	16.3	78.5	-6.6	14.9
ARM SGP E08	1.1	22.5	1.5	7.1	9.2	81.5	-7.6	15.9
ARM SGP E09	1.2	22.8	2.0	7.1	7.7	84.7	-8.4	15.9
ARM SGP E10	5.9	21.3	1.7	7.4	14.8	88.5	-1.8	17.1
ARM SGP E11	-1.1	25.2	2.4	7.2	6.2	83.4	-6.2	15.0
ARM SGP E12	6.4	20.3	2.3	7.3	12.2	88.7	-2.3	15.9
ARM SGP E13	0.6	22.1	2.4	7.4	4.1	84.7	-6.0	16.3
ARM SGP E15	-0.4	22.7	2.3	7.2	3.3	82.7	-5.4	16.3
ARM SGP E16	4.3	19.5	1.1	7.1	9.1	84.4	-5.2	16.1
ARM SGP E18	6.1	23.6	2.0	7.7	8.6	82.1	-26.8#	40.1#
ARM SGP E20	6.5	20.1	1.8	7.5	18.0	73.2	-3.8	14.4
ARM SGP E22	3.3	20.7	1.8	7.3	13.5	82.4	-7.6	15.9
ARM SGP E24	3.7	19.7	1.9	7.0	6.9	78.0	-0.7	14.4
ARM TWP Manus MAN	11.8	22.7	-2.0	7.8	3.8	180.0	-1.8	10.5
ARM TWP Nauru NAU	7.7	21.3	-2.6	7.3	54.3#	159.5#	-5.4	10.2
CMDL Bermuda BER	24.7	21.8	-0.3	6.6	25.9	143.4	-1.7	15.5
CMDL Kwajalein KWA	7.4	20.2	-1.7	7.5	12.9	133.9	-0.8	10.4
CMDL Samoa SAM	4.5	22.7	-2.2	6.8	20.3	136.5	-1.8	10.5
CMDL Barrow BAR	3.2	16.2	3.4	8.2	4.6	71.9	1.8	23.9
CMDL South Pole SPL	16.4	13.2	3.3	7.3	-8.2	33.4	14.1	28.6
CMDL Boulder, Co BOU	1.1	19.4	-1.2	6.8	9.9	125.0	-13.0	17.3
BSRN Tateno, Jp TAT	10.7	30.6	-0.9	6.6	24.4	92.8	-6.5	13.4
BSRN Alice Springs, Au ASP	8.0	21.6	-0.3	6.3	15.0	77.2	-16.5	15.8
BSRN Syowa, Ant SYO	3.1	14.4	-0.7	6.9	21.2	61.9	-9.0	32.8
BSRN Georg von Neumayer,Ant GVN	6.5	12.7	2.6	8.5	0.1	46.4	-4.3	32.9
BSRN Ny Ålesund,Spitsbergen NYA	5.8	14.9	1.2	7.5	14.4	62.9	-5.0	26.9
BSRN Payern,Swiss PAY	4.4	22.7	0.9	6.2	34.3	126.2	-12.3	18.3
BSRN Lindenberg, Ge LIN	4.8	21.8	1.3	6.2	-4.2	86.9	1.7	17.1
BSRN Sede Boqer, Israel SBO	-7.3	26.2	1.2	6.0	8.9	88.4	-0.7	23.8
BSRN De Aar, South Africa DAA	2.7	13.9	0.8	6.5	24.2	75.7	-18.4	15.4
BSRN Lauder, New Zealand LAU	4.3	19.0	-0.4	5.8	15.4	123.2	-13.6	22.0
BSRN Tamanrasset, Algeria TAM	6.4	23.9	-2.2	8.5	-5.1	69.7	5.0	13.8
Chesapeake Light, VA COV	19.0	22.6	1.8	8.1	-8.4	74.9	12.4	16.8
Saudi Solar Village, SSV	-0.9	15.4	-1.6	7.1	-2.7	47.7	-2.0	13.3
Valancia Anchor Station, Spain VAS	9.7	22.6	1.4	6.3	0.7	93.1	-5.6	20.4
ALL Stations (All Sky)	**5.4**	**21.1**	**1.2**	**7.4**	**9.7**	**89.7**	**-4.2**	**21.5**
ALL Stations (CLEAR)	***0.6***	***9.4***	***0.0***	***4.7***	***1.2***	***23.7***	***-8.2***	***15.6***

Table 2: Proto-Ed3 Fu Model *minus* Observations over a 64-month period. Toa flux observations from CERES Ed2 CRS, Surface observations from CAVE (Ceres Arm Validation Experiment) a collection of 30minute averaged surface flux observations from several groups (SURFRAD, BSRN, CMDL and independent stations) (# Suspect bad data not included in summary of "All Stations") Clear Sky according to CERES MODIS TOA cloud mask.

5. References

Bodhaine, B.A, 1999: On Rayleigh Optical Depth Calculations, *J. of Atmos. Ocean. Tech*. Vol. 16 1854-1861

Charlock, T. P., and T. L. Alberta, 1996: The CERES/ARM/GEWEX Experiment (CAGEX) for the retrieval of radiative fluxes with satellite data*. Bull. Amer. Meteor. Soc.,* 77, 2673-2683

Charlock, T. P., F. G. Rose, D. A. Rutan, Z. Jin, and S. Kato, 2006: The Global Surface and Atmosphere Radiation Budget: An Assessment of Accuracy with 5 years of Calculations and Observations. Proceedings of 12th Conference on Atmospheric Radiation (AMS), 10-14 July 2006, Madison, Wisconsin.

Collins, W.D., P.J. Rasch, B.E. Eaton, B.V. Khattatov, J.-F. Lamarque, and C.S. Zender, 2001: Simulating aerosols using a chemical transport model with assimilation of satellite aerosol retrievals Methodology for INDOEX. *J. Geophs. Rev*. 106, 7313-7336

d'Almeida, G. A., P. Koepke, and E. P. Shettle, 1991: Atmospheric aerosols - global climatology

and radiative characteristics*. A. Deepak Publishing, Hampton, Va*, 561 pp.

Hu,Y.X and Stamnes,K 1993: An Accurate Parameterization of the Radiative Properties of Water Clouds Suitable for Use in Climate Models*, Journal of Climate*: Vol. 6, No. 4, pp. 728-742.

Fu, Q., and K.-N. Liou, 1992: On the correlated k-distribution method for radiative transfer in nonhomogenous atmospheres*. J. Atmos. Sci*., 49, 2139-2156.

Fu, Q, 1996: An accurate parameterization of the solar radiative properties of cirrus clouds for climate models, J Clim. Vol 9, 2058-2082

Jin, Z., and K. Stamnes, 1994: Radiative transfer in nonuniformly refracting layered media: Atmosphere ocean system. Appl. Opt., 33, 431 442.
.
Kato, S., T. P. Ackerman, J. H. Mather, and E. E. Clothiaux, 1999: The k-distribution method and correlated-k approximation for a Shortwave Radiative Transfer Model, *J. Quant. Spectrosc. Radiat. Transfer*, 62 ,109-121

Kato, S., F.G., Rose, and T.P., Charlock, 2005: Computation of Domain-Averaged Irradiance Using Satellite-Derived Cloud Properties, *J. of Atmos. Ocean. Tech*., 22b, pp 146-164.

M. Hess, P. Koepke, and I. Schult, 1998: Optical Properties of Aerosols and clouds: The software package OPAC, *Bull. Am. Met. Soc*., Vol. 79, 831-844

Ohmura A., E. Dutton, B. Forgan, C. Frohlich, H. Gilgen, H. Hegne, A., Heimo, G., Konig-Langlo, B. McArthur, G. Muller, R. Philipona, C. Whitlock, K. Dehne, and M. Wild, 1998: Baseline Surface Radiation Network (BSRN/WCRP): New precision radiometery for climate change research. Bull. Amer. Meteor. Soc., Vol. 79, No. 10, 2115-2136

Rose, F., T. Charlock, B. Wielicki, D. Doelling, and S. Zentz, 2006: CERES Synoptic Gridded Diurnally Averaged Radiative Transfer. Proceedings of 12th Conference on Atmospheric Radiation (AMS), 10-14 July 2006, Madison, Wisconsin.

Rutan, D.., T. Charlock, F. Rose,, S. Kato, S. Zentz, and L. Coleman, 2006: Global Surface Albedo from CERES/TERRA Surface and Atmospheric Radiation Budget (SARB) Data Product. Proceedings of 12th Conference on Atmospheric Radiation (AMS), 10-14 July 2006, Madison, Wisconsin.

Rutan, D.A., F.G. Rose, N.M. Smith, T.P. Charlock, 2001: Validation data set for CERES surface and atmospheric radiation budget (SARB), WCRP/GEWEX Newsletter, Vol. 11, No. 1, 11-12.

Shettle, F. X. Kneizys, and W. 0. Gallery,1980: Suggested Modification to the Total Volume Molecular Scattering Coefficient in LOWTRAN: Comment, *Appl. Opt.* 19, 2873-2874

Tegen, I., and A. A. Lacis, 1996: Modeling of particle size distribution and its influence on the radiative properties of mineral dust aerosol. *J.Geophy. Res*., 101, 19237-19244.

Wielicki, B.A., B.R. Barkstrom, E.F. Harrison, R.B. Lee, G.L. Smith, and J.E. Cooper, 1996: Clouds and the Earth s Radiant Energy System (CERES): An Earth Observing System Experiment. Bull. Amer. Meteor. Soc., 77, 853-868

6. Acknowledgements

ARM data is made available through the U.S. Department of Energy as part of the Atmospheric Radiation Measurement Program.

CMDL data is made available through the NOAA/CMDL Solar and Thermal Radiation. (STAR) group.

SURFRAD data is made available through NOAA's Air Resources Laboratory/Surface Radiation Research Branch